CSIRO Publishing

International *Journal* of Wildland Fire

Scientific Journal of IAWF

VOLUME 11, 2002

Editor-in-Chief
Dr M Flannigan, Canadian Forest Service, Edmonton, Canada.

International Association of Wildland Fire

IJWF is published for the International Association of Wildland Fire by:

CSIRO PUBLISHING
PO Box 1139 (150 Oxford Street)
Collingwood, Victoria 3066
Australia

Telephone: +61 3 9662 7644 (editorial enquiries)
+61 3 9662 7668 (subscription enquiries and claims)

Fax: +61 3 9662 7611 (editorial enquiries)
+61 3 9662 7555 (subscription enquiries and claims)

Email: publishing.ijwf@csiro.au (editorial enquiries)
publishing.sales@csiro.au (subscription enquiries and claims)

CSIRO PUBLISHING

Please submit all new manuscripts directly to **CSIRO** PUBLISHING, in electronic form only. See the *IJWF* Notice to Authors for more information.

www.publish.csiro.au/journals/ijwf

International Journal of Wildland Fire, 2002, **11**, 193–203

A new method for the analysis of fire spread modeling errors*

Francis M. Fujioka

United States Department of Agriculture, Forest Service, Pacific Southwest Research Station, Riverside, CA 92507, USA. Telephone: +1 909 680 1552; fax: +1 909 680 1501; email: ffujioka@fs.fed.us

This paper is derived from a presentation at the 4th Fire and Forest Meteorology Conference, Reno, NV, USA, held 13–15 November 2001

Abstract. Fire spread models have a long history, and their use will continue to grow as they evolve from a research tool to an operational tool. This paper describes a new method to analyse two-dimensional fire spread modeling errors, particularly to quantify the uncertainties of fire spread predictions. Measures of error are defined from the respective spread distances of the actual and simulated fires at specified points around their perimeters. A ratio error provides a correction factor for the spread model bias. The characteristics of the error are defined by a probability model, which is used to construct error bounds on fire spread predictions. The method is applied to the Bee Fire, which burned 3848 ha on the San Bernardino National Forest, California, in summer 1996. The study focused on the early, presuppression stages of the fire. A mesoscale spectral model was used to simulate weather conditions on a grid interval of 2 km. The FARSITE system was used to simulate fire growth during the first 105 min of the fire. The case study showed how difficult fire spread modeling is under the conditions presented by the Bee Fire.

Additional keywords: Error analysis; confidence limits; mesoscale weather model; FARSITE; error correction.

Introduction

Wildland fire spread models in the USA and elsewhere express the dependence of fire behavior on fuel, weather and topography. Origins of the model favored in the US trace back to Fons (1946), whose work laid the foundation for the Rothermel fire spread model (1972). The Rothermel model has been improved over time (e.g. Albini 1976; Burgan and Rothermel 1984; Andrews 1986) but it, like all fire models, can err significantly in predicting the spread rate of fire. A system is needed to quantify the errors in fire spread models, in terms of magnitude, spatial and temporal variability, and statistical significance with respect to stated hypotheses.

Analyses of fire spread modeling errors are useful for several reasons. First, fire growth patterns can be extremely complex, and are poorly served by the usual one-dimensional methods that focus, for example, on the average or maximum spread rate. Second, we cannot expect to explain fire spread modeling errors completely, hence at some point we should consider their random characteristics. If we can describe the randomness sufficiently, it will be possible to (1) determine statistically significant errors; (2) describe confidence regions for fire growth predictions that contain the true perimeter with specified probability; and (3) simulate the random features of fire growth to provide preparation and insight to deal with real world fire growth.

This study focused on the Bee Fire (Fig. 1), which occurred on the San Jacinto Ranger District of the San Bernardino National Forest, 29 June–3 July 1996. Probably the most remarkable aspect about this fire was that it occurred at a place and time when there was substantial interest in fire spread modeling, and an effort was made to collect data on the environment and growth of the fire for subsequent analysis (Weise and Fujioka 1998).

Attention was paid to the incipient stages of the fire, when fire growth measurements were most frequent, and suppression efforts were minimal to absent. The next section describes the data gathered on the Bee Fire, from which its growth was modeled. The data provided a glimpse of the fire environment, which is described briefly. The third section covers the theory and method of analysis of fire spread simulation errors, followed by the analysis of the Bee Fire simulations. The final section summarizes the main points of the study, and ends with conclusions and recommendations.

10.1071/WF02004 1049-8001/02/030193

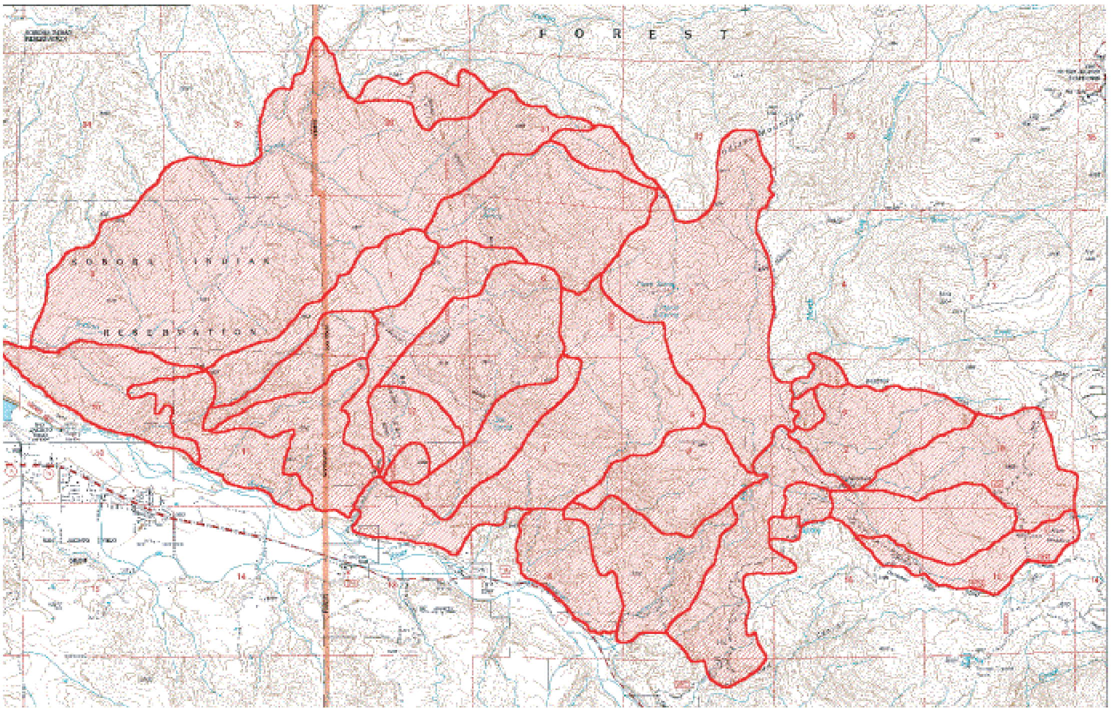

Fig. 1. Map of the Bee Fire, which burned a portion of the San Jacinto Ranger District, San Bernardino National Forest, California, from 29 June to 3 July 1996. The polygons show the various parts of the burn, as they evolved over time.

The Bee Fire

Sources of data

A fire behavior team, consisting of a fire behavior analyst, two trainees, two field observers, a geographic information systems (GIS) specialist and a fire meteorologist generated terrain and fuels data covering the burn site. They obtained weather data for the burn period from a nearby remote automatic weather station (RAWS) at Pine Cove. Through interviews, the team documented information about the sequential growth of the fire in a GIS dataset that described the position of the fire at 28 different times, from 29 June to 3 July 1996 (Fig. 1).

Because the weather data coverage was inadequate, a Forest Service study was initiated, well after the fire, to provide weather data on a 2 km grid spacing for the fire episode, using the so-called Mesoscale Spectral Model (MSM; Chen *et al.* 1998). The weather model, at that resolution, required massive computing resources ordinarily unavailable to a fire behavior team. It is a non-hydrostatic version of the Regional Spectral Model and the Global Spectral Model, which were developed by the National Weather Service (Juang and Kanamitsu 1994). The MSM simulated all of the surface weather variables needed by the fire spread model.

This study examined the first 2 h of the fire, due to limitations of the fire growth data. Within this time span, perimeter data were available at 15, 45, and 105 min after ignition. These were the shortest sampling intervals of the perimeter growth compiled by the fire behavior team. The next perimeter was not be reported until 4.5 h later. Beyond the period of the analysis, the fire did not exhibit the free burning character simulated by our spread model. This may have been due to suppression effects on the fire, faulty documentation of fire growth, modeling deficiencies, or a combination of the above.

Fire environment

The 1996 Bee Fire event started on the afternoon of 29 June, at the base of the San Jacinto Mountains, approximately 1.6 km north-north-west of the Cranston Ranger Station, in the San Bernardino National Forest, California. The ignition point lay in Bee Canyon, from which the fire drew its name (Fig. 2). The fire began at approximately 680 m above sea level and headed generally north-east. The north fork of the San Jacinto River cut through the eastern portion of the burned area, while Indian Creek ran through its western extent. The San Jacinto River bounded the south side of the fire. Chaparral was abundant, the predominant fuel type being chamise (*Adenostema fasciculatum* H&A). Over its life, the Bee Fire threatened multiple resources, including the popular mountain community of Idyllwild, to the east. The suppression team contained the fire after 3 days, but not before the fire covered 3848 ha.

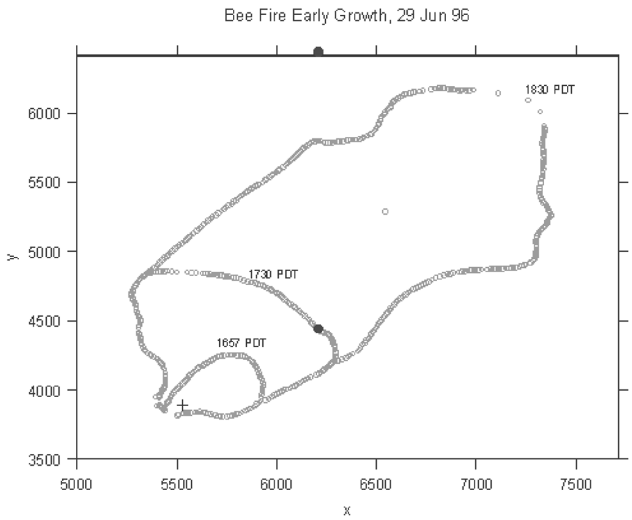

Fig. 2. Plots of the first three perimeters recorded for the Bee Fire, San Bernardino National Forest, California. Axis units are in meters relative to local UTM coordinates. The plus sign indicates the ignition point of the fire. The solid dots are wind model grid points.

The air temperature at the time of ignition, 1647 PDT, was approximately 29°C, relative humidity 19%. Winds blew out of the south-west to north-west at approximately 2 m/s. Less than 2 h later, the temperature dropped to 24°C, and relative humidity increased to 24%. The mesoscale simulations indicated that the breeze from the west was making headway in the area at about the time of ignition. Note in Fig. 3 how the west wind progressed over the landscape from 1500 PDT to 1700 PDT. Starting from the western half, the wind shifted direction by as much as 180°. The mesoscale model also increased the wind speeds, as it turned the winds from easterly to westerly. However, the winds observed near the fire did not confirm an acceleration of the wind flow. Instead, the wind speed held relatively constant at 2 m/s, until 1830 PDT, when it became virtually calm.

The changes in temperature and relative humidity over the period of interest were probably not large enough to induce significant variations in fire behavior. In terms of the corresponding change in equilibrium moisture content of the fuel, a change from 29°C to 24°C (84–75°F), and 19% to 24% relative humidity, makes little difference; in either case, fine dead fuels would be dry. The influence of the wind, on the other hand, can be profound. Because the ignition point was on relatively steep slope (24%) that became even steeper except to the south, a change in wind direction could have altered the fire spread substantially.

Theory and methods of analysis

This section describes a new theory for the spatial analysis of two-dimensional fire spread modeling errors, condensed from Fujioka (2001). It assumes that both simulated and actual fire perimeters can be represented by continuously

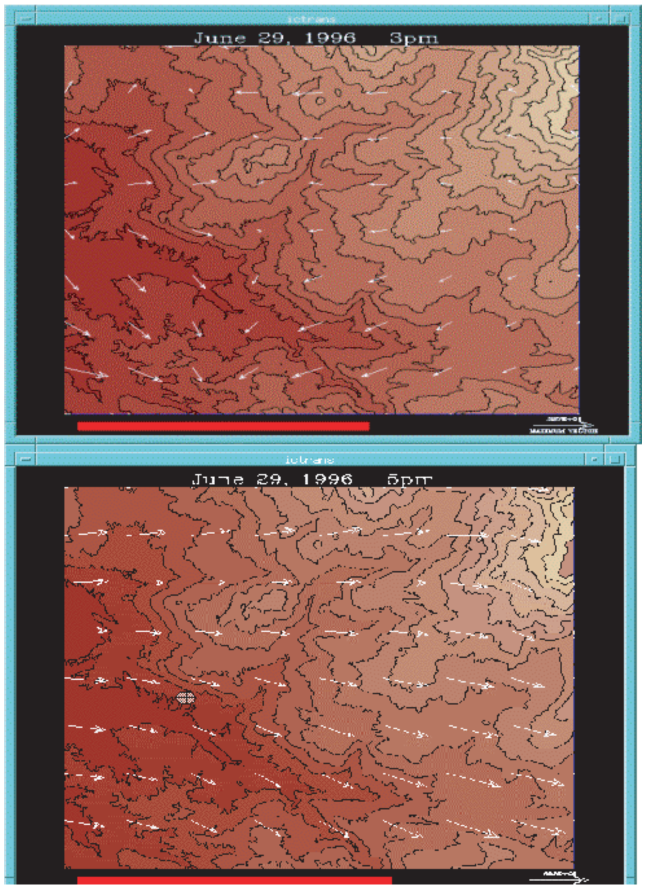

Fig. 3. Mesoscale model simulated winds over the Bee Fire area, at 1500 PDT (top) and 1700 PDT, 29 June 1996. The ignition point was on the west side, approximately at the position indicated by the circle (bottom). The vectors show the wind flow at 10 m above the surface.

differentiable and integrable arcs or closed loops. In this study, the perimeters are represented in polar coordinates, with the origin at the ignition point. Let $r(\theta,t)$ represent the actual perimeter at time t and $R(\theta,t)$ the corresponding simulated perimeter at time t. The simulated perimeters were produced using the FARSITE fire modeling system (Finney 1998) with weather data from the Pine Cove weather station and gridded output from the Mesoscale Spectral Model. I also reran simulations of the first perimeter with trial-and-error modifications to the wind direction observed at Pine Cove at 1657 PDT, because the wind direction of record steered the initial simulated perimeter considerably off course from the observed perimeter. The fire at this stage was small enough that repeated simulations could be done easily and quickly. The significance of the modified wind direction will become apparent in the Results section.

Ideally, r and R are practically indistinguishable for all θ and t. However, mathematical models err for a variety of reasons. Two common types of modeling error cited by Anselin (1989) were measurement error and model specification error. Measurement error occurs, for example, when an observed fire perimeter is improperly located. This kind of error will provide the fire growth model with the wrong initial conditions, or supply incorrect information to verify simulated fire growth. Model specification error includes errors from a model of the wrong functional form or a model with the wrong set of input variables. In this study, these two kinds of errors can occur in several places, because mathematical models are used to simulate weather and fire behavior variables. The many sources of error make the net fire growth modeling error unpredictable. The best we can do is to characterize the error as a random variable, as follows.

Consider two measures of fire spread model error: the difference, D, and the ratio, G, of the radials of observed and simulated fire perimeters:

$$\begin{aligned} D(\theta_j,t) &= r(\theta_j,t) - R(\theta_j,t) \\ G(\theta_j,t) &= r(\theta_j,t)/R(\theta_j,t), \quad R(\theta_j,t) > 0 \end{aligned} \tag{1}$$

Note that G converts to a difference measure if we apply a log transform. The $\{\theta_j\}$ represent the angles at which both simulated and actual perimeter points are available at time t. If a matching simulated point $R(\theta_j,t)$ is missing for any actual point $r(\theta_j,t)$ at time t, one could be obtained by linear interpolation with reasonable precision, because the FARSITE simulations produced a relatively dense set for each time t.

The FARSITE simulator is deterministic, hence $R(\theta,t)$ is deterministic. Make the error measures random variables, by including a random component:

$$\begin{aligned} D(\theta_j,t) &= r(\theta_j,t) - R(\theta_j,t) + \varepsilon(\theta_j,t) \\ \ln\left(G(\theta_j,t)\right) &= \ln r(\theta_j,t) - \ln R(\theta_j,t) + \varepsilon(\theta_j,t) \end{aligned} \tag{2}$$

where, in general, $\varepsilon(\theta_j,t)$ is a zero mean random variable, autocorrelated in both θ and t. For this study, however, assume that the $\{\varepsilon(\theta_j,t)\}$ are independently identically distributed, $\varepsilon \sim F(k)$, where F is some probability distribution with parameter set k. Apply the expectation operator E to both sides of equations (2):

$$\begin{aligned} E\left[D(\theta_j,t)\right] &= E\left[r(\theta_j,t) - R(\theta_j,t)\right] \\ &= B_D(\theta_j,t) \\ E\left[\ln\left(G(\theta_j,t)\right)\right] &= E\left[\ln r(\theta_j,t) - \ln R(\theta_j,t)\right] \\ &= B_{\ln G}(\theta_j,t) \end{aligned} \tag{3}$$

Correction for simulation bias

The functions B_D and $B_{\ln G}$ represent bias in the fire spread simulations. They are estimated from the simulated and observed fire spread. Like the spread functions from which they are derived, the bias functions are also assumed to be smooth in a mathematical sense. Ideally, the spread model is unbiased, and B is zero for all θ and t. However, if the spread model is biased, the bias estimate can be used to correct subsequent fire growth simulations, assuming the bias is constant from one time step to the next for all θ.

What follows is a generalization of the procedure described by Rothermel and Rinehart (1983) for determining a rate of spread adjustment factor derived from the ratio form G of the spread modeling error. Their adjustment factor focused on the head fire spread rate, whereas the following procedure describes an adjustment factor that varies around the perimeter of the fire. The latter is needed in FARSITE (Finney 1998), particularly when fire exhibits high frequency variability in space and time.

After determining the bias in the form of G, use the observed perimeter as the initial fire position for the next iteration. Let t_2 denote the next time step in the simulation, when the correction for the fire spread modeling bias will be applied. Calculate the corrected growth, R_C, at t_2 by scaling the spread model estimate in proportion to G:

$$R_c(\theta,t_2) = R(\theta,t_2)G(\theta,t) \tag{4}$$

From equation (2), the error of the corrected estimate is

$$\begin{aligned} \ln G_C(\theta,t_2) &= \ln r(\theta,t_2) - \ln R_C(\theta,t_2) + \varepsilon(\theta,t_2) \\ &= \ln r(\theta,t_2) - \ln R(\theta,t_2) - \ln G(\theta,t) + \varepsilon(\theta,t_2) \end{aligned} \tag{5}$$

Assuming constancy of the bias in the spread estimates, the expected value of $\ln G_C$ is

$$\begin{aligned} E\left[\ln G_c(\theta,t_2)\right] &= E\left[\ln r(\theta,t_2) - \ln R(\theta,t_2)\right] - E\left[\ln G(\theta,t)\right] \\ &= B_{\ln G}(\theta,t_2) - B_{\ln G}(\theta,t) \\ &= 0 \end{aligned} \tag{6}$$

By comparing the error functions $\ln G_C(\theta,t_2)$ and $\ln G(\theta,t)$, one can visually check the constancy of the bias from one step to the next.

Approximate confidence limits for predicted perimeters

We can construct approximate confidence limits for predicted perimeters from the random characteristics of $\varepsilon(\theta,t)$, in this case the distribution $F(k)$. As equation (2) indicates, ln $G(\theta,t)$ reflects the randomness of $\varepsilon(\theta,t)$: ln $G(\theta,t) \sim F(k)$, under the hypothesis that R is an unbiased estimate of r. Let $g = \ln G$ represent the domain of the real line that F maps to probabilities:

$$P\left\{g(\frac{\alpha}{2};k;t) < \ln r(\theta,t) - \ln R(\theta,t) < g(1-\frac{\alpha}{2};k;t)\right\} = 1-\alpha$$

$$P\left\{\ln R(\theta,t) + g(\frac{\alpha}{2};k;t) < \ln r(\theta,t) < \ln R(\theta,t) + g(1-\frac{\alpha}{2};k;t)\right\} = 1-\alpha$$

$$P\left\{R(\theta,t)\exp\left(g(\frac{\alpha}{2};k;t)\right) < r(\theta,t_2) < R(\theta,t_2)\exp\left(g(1-\frac{\alpha}{2};k;t)\right)\right\} = 1-\alpha \tag{7}$$

The parameters k are easily obtained when G is a lognormal distribution. I used a quantile-quantile plot to check for normality of the log-transformed ratio errors (Venables and Ripley 1994). When the errors did not appear to be normally distributed, I estimated the density of ε using non-parametric density estimation:

$$\hat{f}(x) = \frac{1}{b}\sum_{j=1}^{n} K\left(\frac{x-x_j}{b}\right) \tag{8}$$

where K is a density kernel and b is bandwidth (Silverman 1986; Venables and Ripley 1994). A Gaussian function was chosen for the kernel. The numeric integration of $\hat{f}(x)$ yields F, from which one obtains the quantiles necessary to compute the confidence limits in equation (7).

Spatial resolution of the fire spread simulations

The spatial resolution of the FARSITE simulations are limited by the resolution of the input data, which was as fine as 30 m in this study. Fire growth simulations at this resolution resulted in perimeters with very fine structure, compared with the observed perimeter data. Given that the observed perimeters were reconstructed from interviews, I used a perimeter resolution of 100 m for the simulations, which seemed comparable to the perimeter resolution of the sampled fire data.

Results

Error analysis at 1657 PDT

Figure 4 shows the actual and simulated perimeters at 1657 PDT, 29 June 1996, where the 'Original' weather input for the simulation was obtained from a nearby weather station. At this point, the Bee Fire was about 10 min old. The simulated fire area was smaller than the actual burn, and approximately elliptical. The actual fire perimeter fanned out rapidly toward the north-east. The simulation headed the fire eastward of the actual head fire direction. The error function $G(\theta$, 1657PDT) captured the deficiencies of the simulation as a function of angle around the ignition point (Fig. 5).

An ideal simulation would produce an error curve close to a ratio of 1. At its worst, the actual fire spread to the north-east about 2.6 times faster than the simulation.

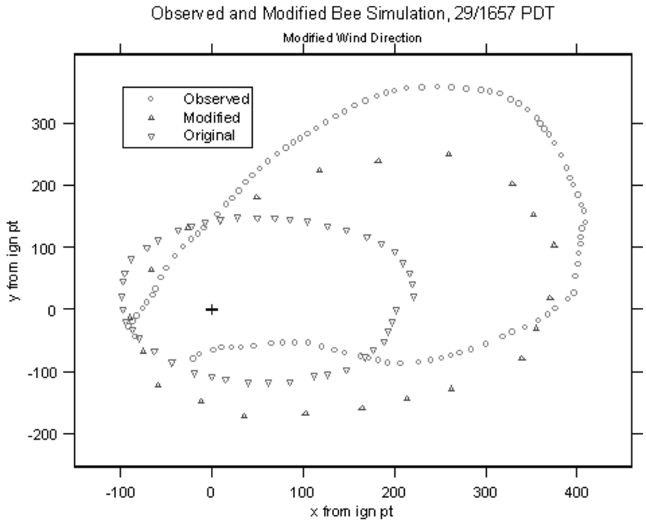

Fig. 4. Bee Fire simulations, 29 June 1996, 1657 PDT, with weather data from Pine Cove (Original), and with the Pine Cove wind direction modified to align the head fire direction of the simulated fire with the observed fire.

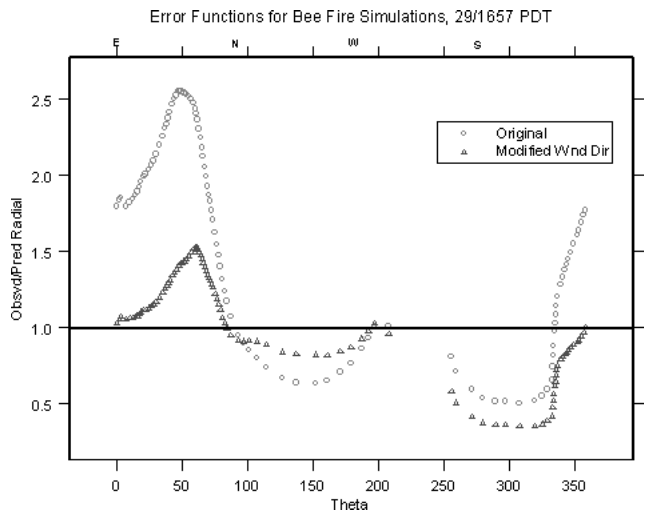

Fig. 5. Errors in the first simulation for the Bee Fire, 29 June 1996, 1657 PDT, expressed as the ratio of observed to predicted radial around the ignition point. Theta points to the east at zero, and increases counterclockwise. Top axis marks corresponding compass points.

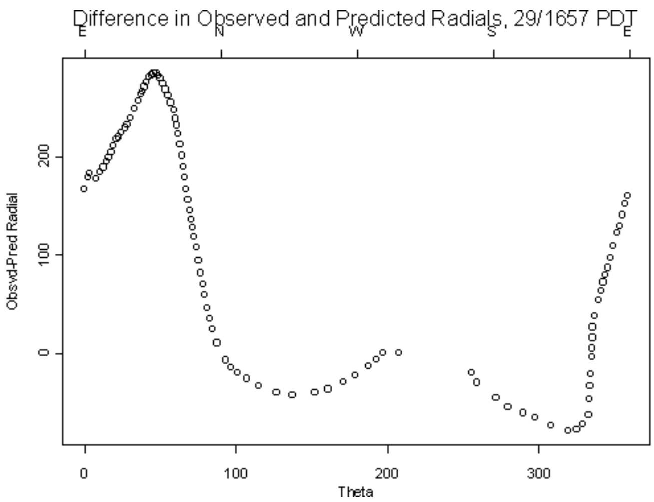

Fig. 6. Simulation error, expressed as the difference between observed and predicted radial lengths, relative to the angle around the ignition point.

Fire growth was overpredicted to the south and north-west, as is evident in the plot of differences (D in equation (1)) between observed and predicted radials (Fig. 6). Note the gap between 210º and 250º, due to the lack of observed perimeter data there.

As stated in the *Theory and methods of analysis* section, I reran the simulation, changing the input wind direction from a compass bearing of 290° to 230° after trial and error, to improve the simulated head fire direction. The result appears in Fig. 5.

The modified wind direction indeed closed the spread between simulated and actual head fire directions. Additionally, it enlarged the area of the simulated burn, particularly toward the north-east. Apparently, the change enhanced the effect of the sloping terrain on fire spread. An unwanted side effect of the modification was a further overprediction on the south side of the fire. The modification reduced the error ratio in the head fire direction by approximately 40%.

The fire growth simulation at 1657 PDT was repeated with winds from the mesoscale model initialized by synoptic weather data from 28 June 1996, 1700 PDT (Fig. 7). The mesoscale model winds predicted for the afternoon of 29 June (e.g. Fig. 3) overpredicted the observed wind speeds. As a result, the simulated spread rate was much higher than what was observed.

Error analysis at 1730 PDT

The error analysis from 1657 PDT provides the information necessary to correct for model bias in the next step fire spread prediction. The target prediction time was 1730 PDT, the observation time of the next fire perimeter. I used the error analysis from 1657 PDT of the simulation incorporating the modified wind direction, which gave the best result. Figure 8 shows three different simulations and the actual fire perimeter at 1730 PDT.

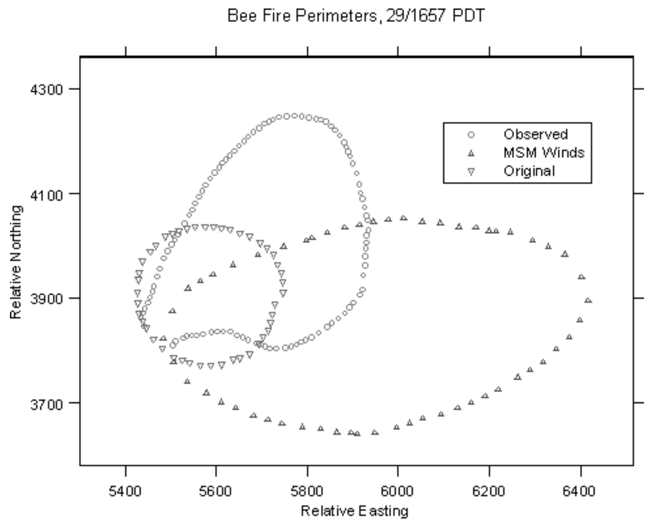

Fig. 7. Observed and simulated Bee Fire perimeters on 29 June 1996, 1657 PDT. The perimeter plot marked 'MSM Winds' was simulated with wind input from the Mesoscale Spectral Model with initial data from 28 June 1996, 1700 PDT. The 'Original' perimeter is from the initial simulation in Fig. 4.

The 'Uncorrected' perimeter in Fig. 8 was obtained from the simulation starting at the ignition point, with the modified wind direction. The 'Position Corrected' perimeter was the simulation beginning at 1657 PDT, initialized by the perimeter observed at that time. The 'Position + Bias Corrected' simulation utilized not only the updated perimeter information, but also the bias evaluated at 1657 PDT, $G(\theta,1657)$.

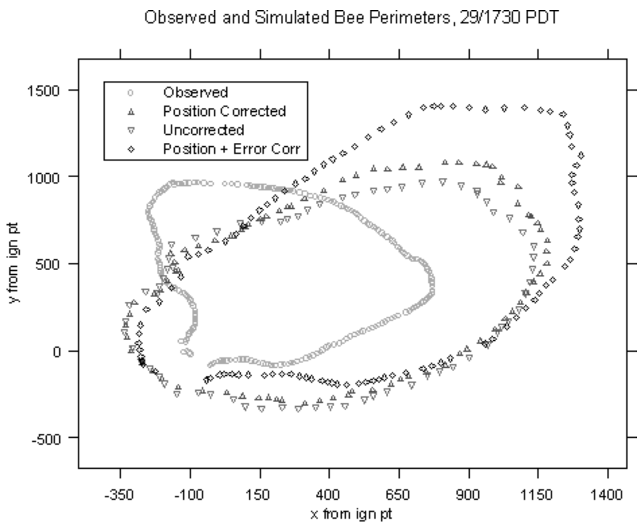

Fig. 8. Observed and simulated Bee Fire perimeters, 29 June 1996, 1730 PDT. Corrected perimeters use error information from the perimeter observed at 1657 PDT.

None of the corrected simulations seemed to improve upon the 'Uncorrected' one. All of the simulations overestimated the spread to the east, and underestimated the spurt of the actual fire to the north-west, reflected in Fig. 9 as a pronounced peak for theta of about 100º. As indicated in both Figs 8 and 9, the simulations mostly overestimated the actual fire at 1730.

The marginal performance of the fire spread simulations to this point underscores the need for an uncertainty analysis, at least to describe a region of space wherein the true perimeter might lie, with specified probability. This requires knowledge of the distributional properties of the spread model error, as outlined in the section on theory and methods. I checked for normality of the ratio error G in the error analysis at 1657 PDT.

Figure 10, a quantile-quantile plot (Venables and Ripley 1994), provides a check of normality of the ratio of observed and predicted radials for the fire perimeters at 1657 PDT. If the data in question are normally distributed, the plotted points fall along or near the line, which connects the interquartile points. The middle points in Fig. 10 fell along or near the line, but sharp deviations occurred in the tails. I applied a log transform to the ratios and estimated their resultant probability density.

Figure 11 is a non-parametric density estimate (Silverman 1986; Venables and Ripley 1994) of the log ratio measure of error for the Bee Fire simulation at 1657 PDT. The estimated density was hardly close to Gaussian, and it appeared that changing either the kernel function or bandwidth could not make it more so. Hence, there was little evidence that the spread model errors were normally distributed.

I therefore formed an empirical distribution function from the non-parametric density estimate of the log ratio errors, and obtained the quantiles corresponding to a 95% confidence interval for the actual fire perimeter at 1730 PDT (Fig. 12). However, the confidence limits did not contain the unexpected growth of the actual fire to the north-west.

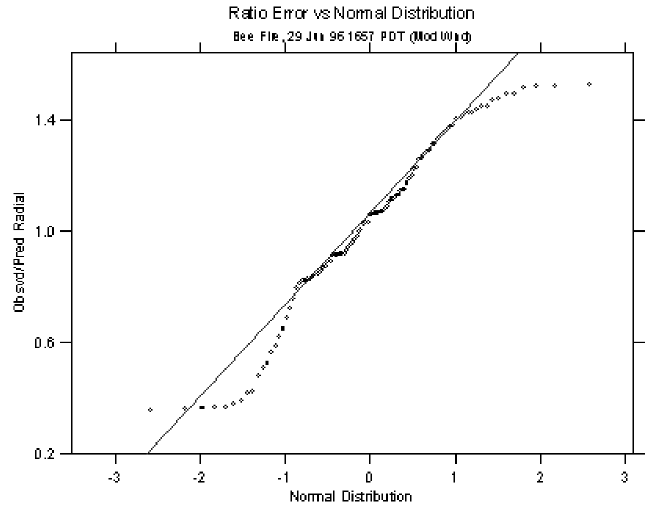

Fig. 10. Quantile-quantile plot of the ratio measure of error for the Bee Fire simulation with modified wind direction, 29 June 1996, 1657 PDT.

Error analysis at 1830 PDT

The error analysis at 1830 PDT is an iteration of the procedure just described for 1730, with a fresh update on the spread model error characteristics for the prediction at 1830. Figure 13 shows the position corrected simulation that started from the observed fire position at 1730. Also shown for comparison is the predicted perimeter generated from the ignition point, from the same simulation that produced the modified perimeter in Fig. 4, and the uncorrected perimeter in Fig. 8.

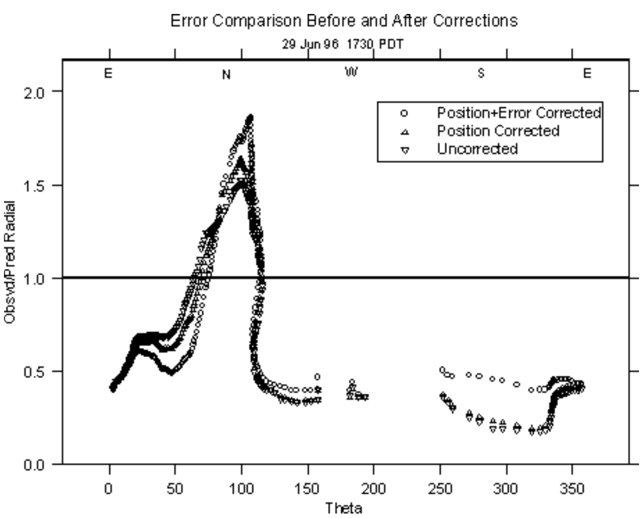

Fig. 9. Ratio form of error function for simulations in Fig.12, as evaluated by comparison to the perimeter observed on 29 June 1996, 1730 PDT.

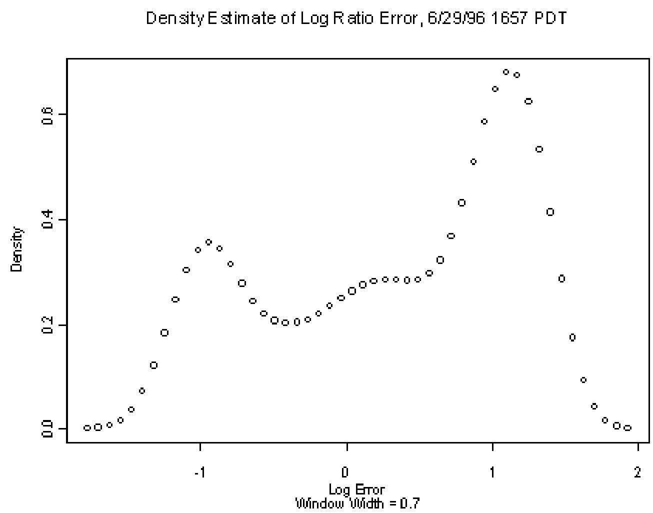

Fig. 11. Non-parametric density estimate of the log ratio of observed to predicted radials for the Bee Fire simulation with modified wind direction, 29 June 1996, 1657 PDT.

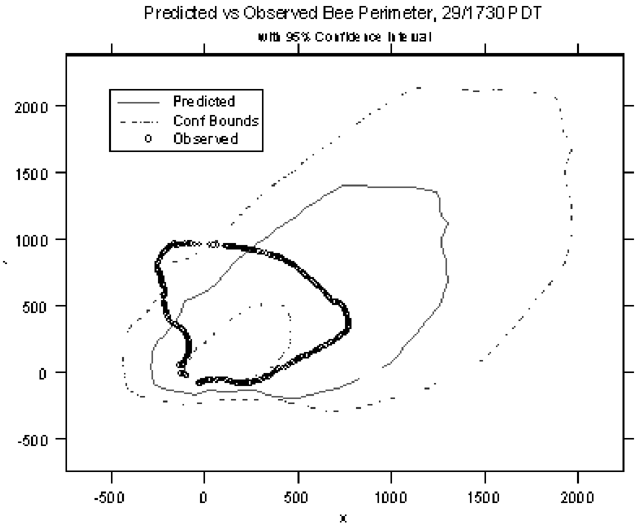

Fig. 12. Position and bias corrected perimeter prediction for the Bee Fire, 29 June 1996, 1730 PDT, and approximate 95% confidence interval for the true perimeter.

The fully corrected simulation, incorporating both position and bias information from 1730, was harder to develop. The problem arose from the concavity in the ratio error function near theta equals 110° (Fig. 9). The polar coordinate geometry ordered the points in theta sequence, and as a result mixed the spatial order that the points occurred in, going counterclockwise around the perimeter. This happened because the concavity placed points behind one another, relative to the ignition point. Hence, large radial values were interspersed among small ones, creating uncharacteristic high frequency variations in an otherwise smooth function. I implemented a spline smoothing function in this region (Chambers and Hastie 1992), to dampen the variability. The result (Fig. 14) was still not very smooth, because of the number of points that the concave region contained.

As before, I checked for normality of the errors using quantile-quantile plots (not shown). In all cases, the tails of the distribution were heavy, particularly the lower tails. The ratio form of the error function departed significantly from the straight line that would attract the points from a normal distribution. The log transform of the ratio reduced the departures, but not substantially. I therefore estimated the empirical distribution of the errors (Fig. 15), to obtain the confidence region on the predicted perimeter.

The non-parametric density estimate of the log ratio error for 1730 gave a modal value indicative of overprediction, but this was balanced somewhat by an extended right tail. An approximate 95% confidence interval was obtained from the log error ratio quantiles at (–0.81, 0.82) of the empirical distribution function. This yielded the corresponding prediction and 95% confidence region for the perimeter at 1830 PDT that appear in Fig. 16.

The perimeter prediction at 1830 PDT overestimated the growth to the north-west, and underestimated the growth to the north-east. The simulated surge to the north-west was influenced by the underprediction in that direction at 1730 PDT. The actual fire pushed further in the north-east direction than the trend at 1730 indicated. The broad confidence region to the north-west was a reflection of the uncertainty in this part of the fire. Figure 17 compares the error function for this prediction with the other simulations for 1830.

Before analysing the perimeter data at 1830, I relocated the polar coordinate origin to the centroid of the actual perimeter at 1830, in an attempt to circumvent the

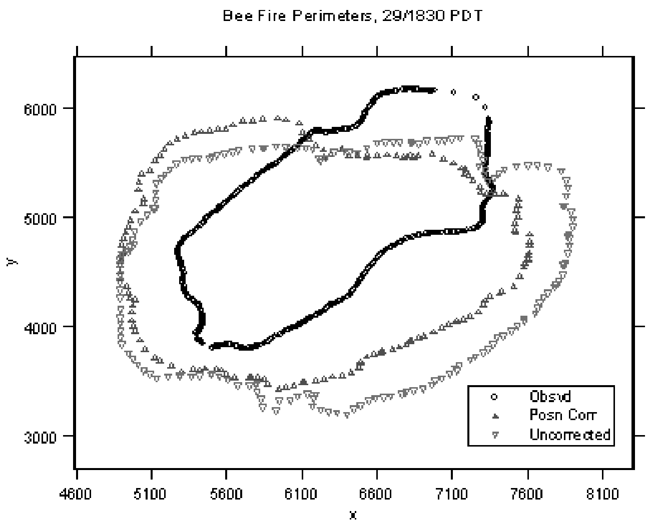

Fig. 13. Simulated and observed Bee Fire perimeters at 1830 PDT, 29 June 1996. The 'Uncorrected' simulation was generated from the initial modified Pine Cove winds.

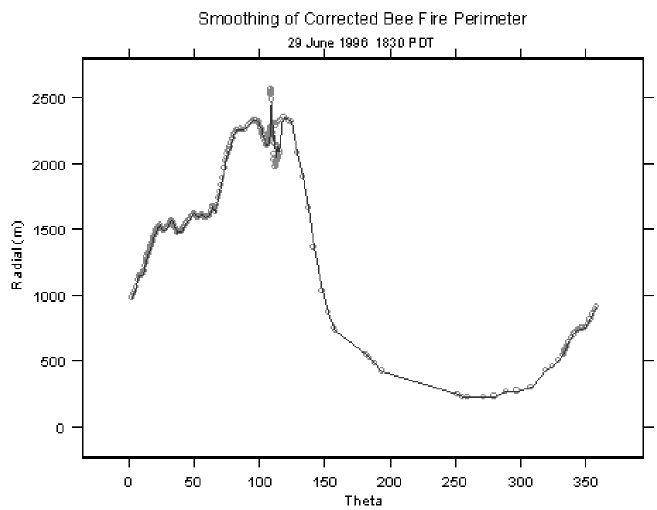

Fig. 14. Position and bias corrected simulation of Bee Fire perimeter at 1830 PDT, in polar coordinate form. The line plot shows a spline-smoothed version of the points plot.

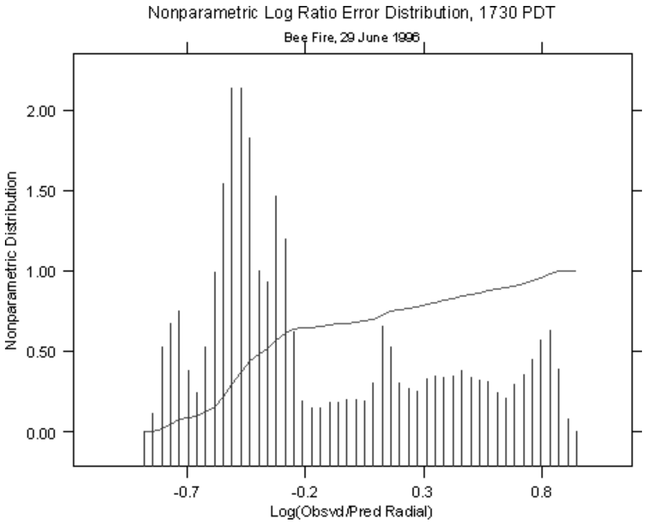

Fig. 15. Non-parametric density estimate (needle plot) and corresponding cumulative distribution of the log ratio error function obtained from the analysis of the Bee Fire simulation at 1730 PDT, 29 June 1996.

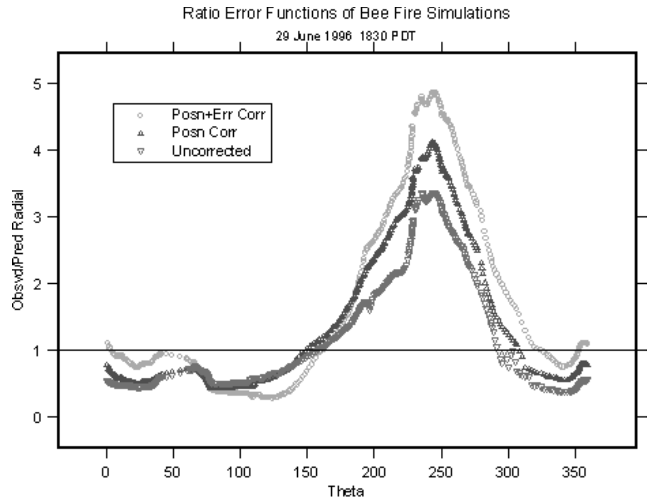

Fig. 17. Comparison of ratio error functions of the Bee Fire simulated perimeters at 1830 PDT, 29 June 1996. Note that the polar coordinate origin now passes through the centroid of the actual perimeter at 1830 PDT.

concavity problem encountered earlier. Figure 17 shows that the fully corrected simulation produced the worst underestimates, although it was slightly better for the theta range from approximately 320º to 70º. None of the simulations came close to the spread of the actual fire for theta near 250º.

Discussion

The characteristics of the fire spread simulation errors merit closer inspection of the wind and slope effects. Although the wind speeds observed and modeled during the Bee Fire were not great, the influence of wind direction was, or could have been significant. The slope of the terrain can enhance or suppress the wind effects, depending on whether the wind blows the fire uphill or downhill. I therefore isolated the slope effect, by simulating the Bee Fire with no wind (Fig. 18).

In the absence of wind—all the other factors of the fire environment unchanged—FARSITE did not at any time grow the Bee Fire to the extent the actual fire grew. Moreover, the actual fire headed toward the north-east substantially more than the no-wind simulation, while the latter tended to grow

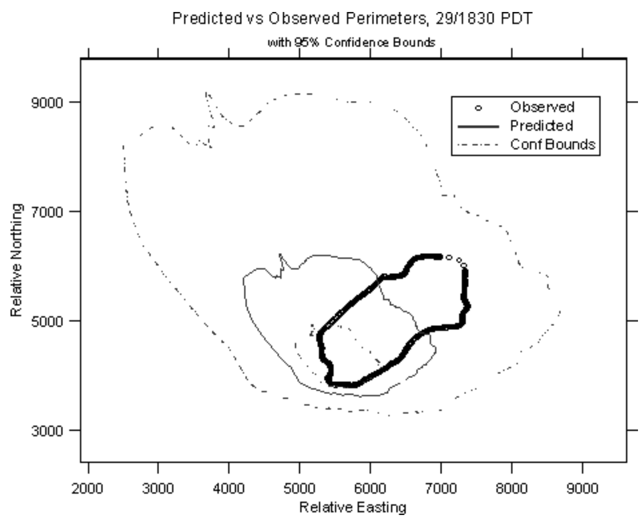

Fig. 16. Simulated and observed Bee Fire perimeters at 1830 PDT, 29 June 1996. The 95% confidence region was generated from quantiles estimated from a nonparametric estimate of the error distribution.

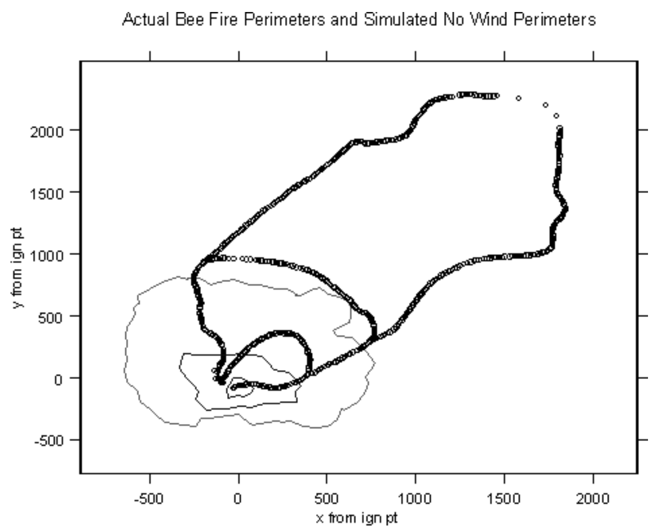

Fig. 18. Comparison of the actual Bee Fire perimeters and the corresponding simulated perimeters under a no wind scenario.

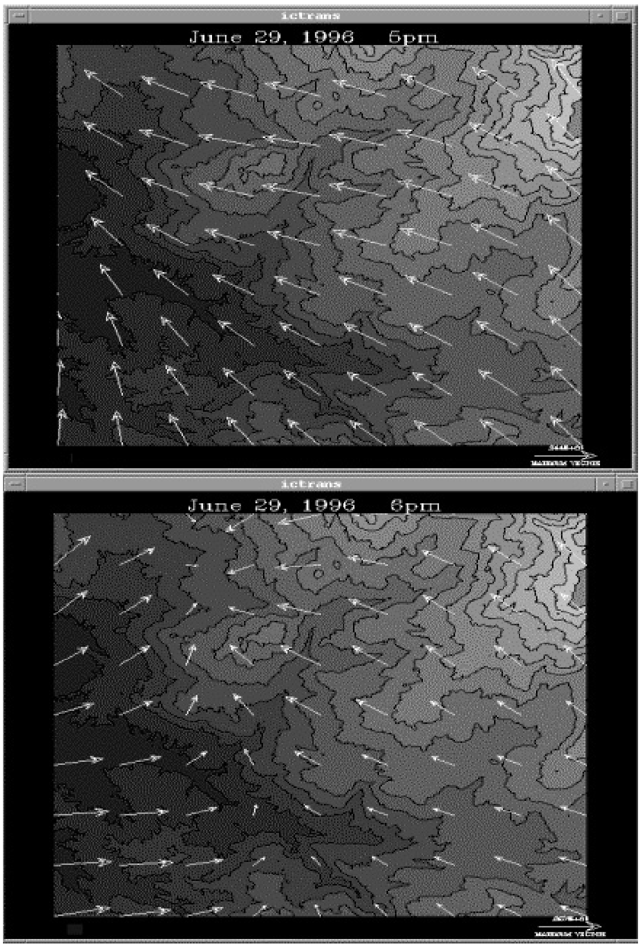

Fig. 19. Mesoscale model analysis of Bee Fire winds on 29 June 1996.

more to the west and south-west than the actual fire. The simulated no-wind fire grew least to the south; the actual fire had no growth to the south, beyond the perimeter at 1657 PDT. A wind from the south-west is therefore a plausible mechanism to replicate the actual fire growth. A south-west wind would spread the simulation more to the north-east, and retard the fire growth toward the south-west.

Now compare the mesoscale model *analysis* in Fig. 19, based on data obtained on 29 June 1996 at 1700 PDT, with the mesoscale model *forecast* in Fig. 3, based on data from 28 June 1996 at 1700 PDT. The latter predicted winds from the west to west-north-west in the burn area at 1700, while the former depicted winds in transition from a south-easterly flow to a westerly to south-westerly flow from 1700 to 1800 on 29 June. The analysis on 29 June provides plausible evidence, therefore, of south-westerly winds that would direct the fire toward the north-east. Using this wind dataset in FARSITE produced the simulated perimeter at 1730 in Fig. 20.

The FARSITE simulation with the analysed mesoscale model winds did the best of all the simulations at 1730 PDT in reproducing the fire spread to the north and north-east. Both

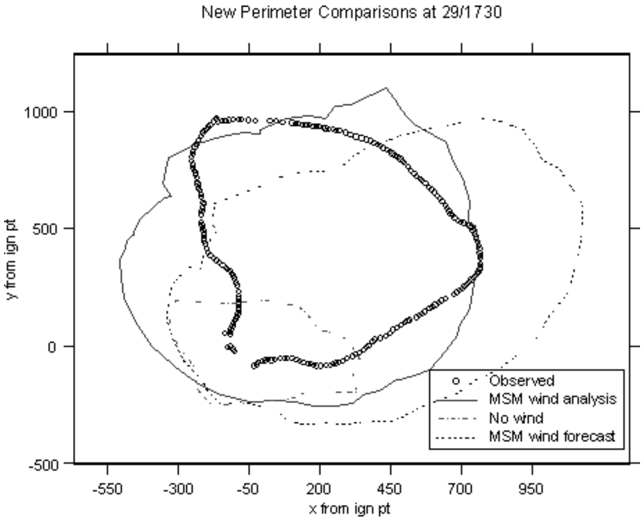

Fig. 20. Observed and simulated perimeters for 29 June 1996, 1730 PDT. MSM refers to the Mesoscale Spectral Model used in this study.

overprediction and underprediction errors were reduced, except in the north-western quadrant, where the new simulation overestimated the actual growth more than the other simulations. All of the simulations, including the one with no wind, overestimated growth in the western through south-eastern quadrants. The actual fire showed little to no growth there.

The perimeter observed at 1830 PDT was more difficult to reproduce, even in retrospect. By trial and error, I tried various combinations of wind directions and low wind speeds, using both the mesoscale model analysis and artificial uniform wind fields. The simulated perimeter labeled 'MSM wind analysis' in Fig. 21 was one of the better model runs for 1830 PDT. Note that the actual fire had the

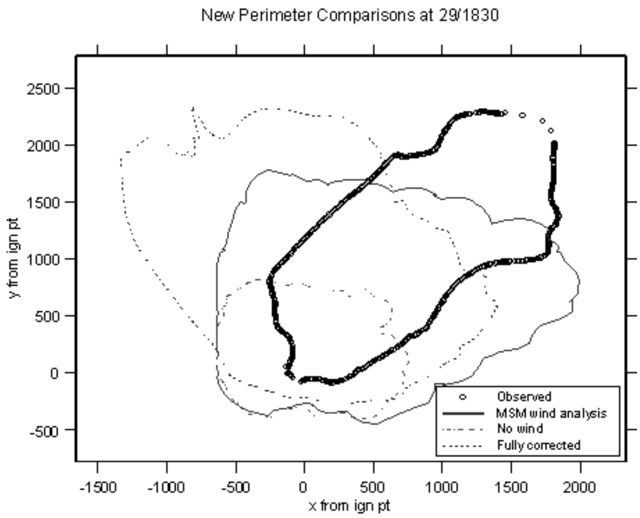

Fig. 21. Observed and simulated perimeters for 29 June 1996, 1830 PDT. The fully corrected perimeter is from Fig. 20.

narrowest profile along the heading direction (south-west to north-east). By comparison, all of the simulations tended to stretch the fire more in the west and east direction, including the no wind simulation.

Summary and Conclusions

This paper demonstrated a new method for two-dimensional analysis of fire spread modeling errors. The method compared the respective spread distances of the actual and simulated fires at common azimuths around their perimeters. Error was expressed as the difference in spread distances, and as the ratio of spread distances, from one time period to the next. The ratio measure also provided a correction factor for the next step prediction. An analysis of the error distribution was used to construct a confidence region for the true perimeter.

The method provides a new perspective on spread model error analysis. The results indicate the difficulty of modeling fire spread, even with relatively high resolution mesoscale model wind data. The Bee Fire case exposed some weaknesses in the error analysis. First, the ratio correction did not improve the spread prediction. To the contrary, it magnified the error, when the actual fire changed its spread behavior from one time step to the next. The ratio correction works when the error pattern was consistent between consecutive observations. It could not be expected to work under the circumstances presented by the Bee Fire case study, unless the error characteristics systematically repeated over time. The data at hand did not provide the opportunity to do an extensive study of the temporal variations of the errors. We can conclude, however, that the error functions were different from one time step to the next.

Another weakness in the method was its dependency on polar coordinates, at least for this dataset. Concavity in the Bee Fire perimeter led to misrepresentation of the perimeter data in polar coordinates. A better fire geometry is needed for this situation. One possible solution is to have the simulation program track fire trajectories that emanate from the ignition point. These trajectories can serve the function of the radials, along which we would compare the arc length covered by the actual fire to that covered by the simulated fire (Fujioka 2001).

Errors in the Bee Fire spread simulations did not appear to be Gaussian. Alternatives to normal theory are needed for the error analysis. The empirical distribution function of the errors provided the information necessary to generate confidence regions. Further investigation may improve the techniques applied here.

The grid spacing of the mesoscale meteorological model simulations was probably too coarse for this case study of the Bee Fire. A denser network of weather stations was also sorely lacking. The data in this study were too limited to exercise completely the potential combination of a high resolution weather model and fire spread model. More frequent observations of the actual fire perimeter are needed to test the capabilities of the weather/fire modeling system. However, the fact that a simple modification in the wind direction led to a considerable improvement in the fire spread simulations illustrates the importance of weather information to the accuracy of the model output.

Finally, we have completely ignored the spatial autocorrelations of the errors. Clearly, the errors were not random functions of space (of theta, for example). When such correlations exist, they must be accounted for in terms of autocovariance functions of space. Random field theory provides a comprehensive approach for the purpose (Fujioka 2001). It also poses the challenge of a steep learning curve. This is the subject of a future paper.

References

Albini FA (1976) Computer-based models of wildland fire behavior: a user's manual. USDA Forest Service. Ogden, UT. 68 pp.

Andrews PL (1986) BEHAVE: fire behavior prediction and fuel modeling system–BURN subsystem, Part 1. USDA Forest Service, Intermountain Research Station General Technical Report INT-194. Ogden, UT.130 pp.

Anselin L (1989) What is special about spatial data? Alternative perspectives on spatial data analysis. In 'Symposium on spatial statistics, past, present and future'. pp. 63–80. (Syracuse University: New York)

Burgan RE, Rothermel RC (1984) BEHAVE: fire behavior prediction and fuel modeling system–FUEL subsystem. USDA Forest Service, Intermountain Research Station General Technical Report INT-167. Ogden, UT. 126 pp.

Chambers JM, Hastie TJ (1992) 'Statistical models in S.' (Wadsworth and Brooks: Pacific Grove, CA)

Chen S-C, Roads JO, Juang H-MH (1998) Mesoscale fire weather studies. In 'Proceedings, Second Conference on Fire and Forest Meteorology', Phoenix, AZ, pp. 134–135. (American Meteorological Society: Boston, MA)

Finney MA (1998) FARSITE: Fire Area Simulator—model development and evaluation. USDA Forest Service, Research Paper RMRS-RP-4. Ogden, UT. 47 pp.

Fons W (1946) Analysis of fire spread in light forest fuels. *Journal of Agricultural Research*, **72**, 93–121.

Fujioka FM (2001) Characterization and analysis of fire spread modeling errors in an integrated weather/wildland fire model. Ph.D. dissertation, University of California, Riverside.

Juang H-MH, Kanamitsu M (1994) The NMC nested regional spectral model. *Monthly Weather Review* **122**, 3–26.

Rothermel RC (1972) A mathematical model for predicting fire spread in wildland fuels. USDA Forest Service, Research Paper INT-115. Ogden, UT. 40 pp.

Rothermel RC, Rinehart GC (1983) Field procedures for verification and adjustment of fire behavior predictions. USDA Forest Service, General Technical Report INT-142. Ogden, Utah. 25 pp.

Silverman BW (1986) 'Density estimation for statistics and data analysis.' (Chapman and Hall: London)

Venables WN, Ripley BD (1994) 'Modern applied statistics with S-Plus.' (Springer-Verlag: New York)

Weise DR, Fujioka FM (1998) Comparison of fire spread estimates using weather station observations versus nested spectral model gridded weather. In 'Proceedings, Second Conference on Fire and Forest Meteorology', Phoenix, AZ, pp. 75–79. (American Meteorological Society: Boston, MA)